Kinetic Isotope Effect on the Photoenolization of *o*-Methylanthrone. A Microcanonical Transition State Theory Calculation

Ricard Casadesús, Miquel Moreno,* and José M. Lluch

Departament de Química, Universitat Autònoma de Barcelona, 08193 Bellaterra, Barcelona, Spain

Received: January 13, 2004; In Final Form: March 8, 2004

The photoenolization of 1,4-dimethylanthrone (1,4-MAT) and 1,4-dimethylanthrone-d_8 (1,4-DMAT) in the gas phase and in 2,2,2-trifluoroethanol (TFE) has been studied theoretically in this work. An electronic energy profile with minima and saddle-point structures is determined by density functional theory methods in the ground state (S_0) and in the triplet state (T_1). This study reveals that in the excited state an inversion of stability of the tautomers and a lower energy barrier to overcome makes the proton transfer feasible. Our molecular orbital analysis shows that upon proton transfer, T_1 changes from n,π* to π,π* so that a diabatic crossing takes place along the reaction coordinate. This crossing is not influenced by the presence of TFE. Also, upon the photoexcitation to the first excited singlet state (S_1) an intersystem crossing must occur to access T_1. Pure electronic calculations cannot tell us the exact point of the triplet potential energy surface that will be accessed. For this reason we have performed a microcanonical dynamic calculation taking into account the tunneling effect of the hydrogen and deuterium transfer rate constants (k_H and k_D, respectively) on T_1. After the rate-constant calculation we have also calculated the kinetic isotope effect (KIE) to compare with the experimental value. Our results indicate that the predicted large KIE for this reaction can be explained if the proton transfer takes place through tunneling at an energy slightly below the barrier.

Introduction

The study of chemical reactivity in electronically excited states is a challenging task both experimentally and theoretically. After the absorptive act the electronically excited molecule can rearrange or fragment (photochemical reaction) or can lose its excitation energy to return to the ground state (photophysical process). A number of different physical unimolecular de-excitation pathways is possible. Fluorescence and phosphorescence, depending on whether the spin multiplicity is retained or not along the transition, respectively, are radiative processes that involve the emission of electromagnetic radiation. In turn, radiationless processes involve the conversion of one molecular quantum state to another at constant energy without emission of radiation. Internal conversion (IC) and intersystem crossing (ISC), respectively, correspond to an allowed transition between electronic states of the same spin multiplicity or a forbidden transition between electronic states of different spin multiplicities.[1] In addition, bimolecular or termolecular de-excitations through the energy transfer to other molecules by collisions (thermal decay) can also occur. On the other hand, the electronically excited molecules are often born with some vibrational excitation. In this case, a vibrational relaxation can occur either by collisions with other molecules or, if collisions are infrequent (i.e., in a low pressure gas), by emission of infrared radiation. As a matter of fact, the fate of the electronically excited molecules results from a complicated and competitive interplay of all those possibilities.[2]

A classical example in this field is the photoenolization of *o*-methyl aryl ketones, which has been studied from long time ago.[3−8] The reaction mechanism, illustrated in Scheme 1 for 1,4-dimethylanthrone, is nowadays well established. High yields

SCHEME 1

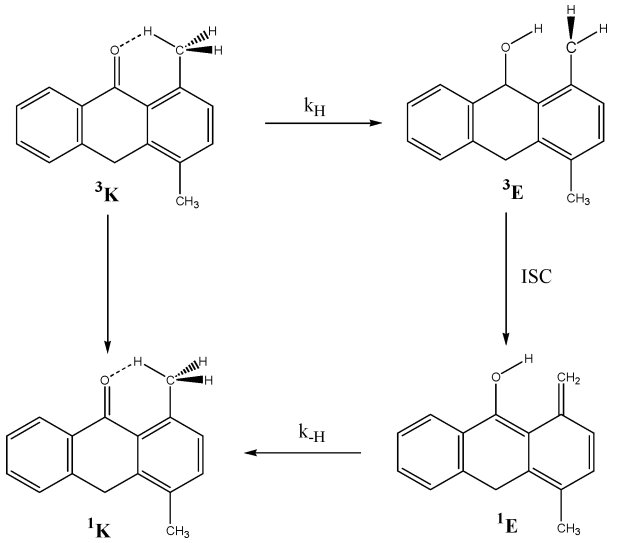

of the triplet ketone ^{3}**K** are formed by a rapid ISC after the initial excitation of the aryl ketone chromophore.[9−12] An adiabatic hydrogen transfer from the *o*-methyl group to the carbonyl oxygen occurs on the triplet surface to give a triplet enol ^{3}**E**, followed by an ISC decay to the ground-state singlet enol ^{1}**E**, which finally reverts to the starting singlet ketone ^{1}**K** through a hydrogen-transfer reaction to complete an overall cyclic process. Several experimental studies with conformationally restricted compounds have concluded that both hydrogen-transfer reactions occur by quantum mechanical tunneling at ultralow reaction temperatures[13−16] (e.g., 4−100 K).

o-Methylanthrones are an especially interesting case. Garcia-Garibay and co-workers have studied experimentally the pho-

* Corresponding author. E-mail: mmf@klingon.uab.es.

10.1021/jp040025a CCC: $27.50
Published on Web 04/21/2004

toenolization of 1,4-dimethylanthrone (1,4-MAT) and 1,4-dimethylanthrone-d_8 (1,4-DMAT) in methylcyclohexane, ethanol, and 2,2,2-trifluoroethanol.[17] They have determined the hydrogen/deuterium-transfer rates of the triplet ketone ^{3}**K** by emission spectroscopy at very low temperatures. These reaction rates were calculated from the total triplet decay rate by subtracting contributions from radiative (phosphorescence) and thermal processes, which were assumed from model compounds lacking the *o*-methyl group (for instance, anthrone or 2,3-dimethylanthrone). They have shown that deuterium transfer of the triplet ketone ^{3}**K** in 1,4-DMAT at very low temperatures (ca. 15−90 K) is slow enough to compete with radiative and thermal decay and so, phosphorescence emission was detected. In the case of 1,4-DMAT in ethanol a curved Arrhenius plot of the total triplet decay rate indicated that deuterium transfer between 18 and 40 K occurs by quantum-mechanical tunneling, with a tunneling rate constant k_D falling between 1.5×10^3 and 7.5×10^3 s^{-1}. This value compares reasonably well with the corresponding rate calculated in methylcyclohexane (2×10^3 s^{-1} between 18 and 30 K). Very interestingly, no phosphorescence emission was observed in the nondeuterated compound 1,4-MAT. Thus Garcia-Garibay and co-workers have suggested that hydrogen transfer of the triplet ketone ^{3}**K** ($k_H \geq 10^7$ s^{-1}) is too fast to allow for phosphorescence to compete with it. Then, the large primary kinetic isotope effect ($k_H/k_D > 10^3$) in the hydrogen/deuterium-transfer rates of the triplet ketone ^{3}**K** would cause an unexpected large isotope effect on phosphorescence emission.

The purpose of this paper is to calculate the hydrogen- and deuterium-transfer unimolecular rate constants of the triplet ketone ^{3}**K** in 1,4-MAT and 1,4-DMAT, respectively, as a function of the energy, to discuss if the kinetic isotope effect (KIE) is large enough to explain the lack of phosphorescence emission in 1,4-MAT. To this aim, we will use electronic structure calculations along with the microcanonical transition state theory. Given the experimental background, quantum mechanical tunneling effects will have to be explicitly calculated.

Theoretical Methods

As we have explained before, we perform electronic and dynamic calculations to describe better the reactivity of *o*-methylanthrones. For this reason we have divided this section into two parts.

Electronic Structure Methods. Density functional theory (DFT) methods have been used in all electronic calculations, and they were performed with the double-ζ quality 6-31G(d) basis set, which includes a set of d-polarization functions on atoms other than hydrogens.[18] For the ground state, geometries and energies were obtained with the B3LYP hybrid density functional.[19] The UB3LYP hybrid density functional was used to optimize the geometries and calculate the energies of the first triplet electronic state. For the first singlet excited state (S_1) calculation we have used the time dependent DFT formalism[20,21] with the B3LYP functional.

Stationary points were located through the minimization procedure of Schlegel by using redundant internal coordinates.[22] The nature of the located stationary points was ascertained by diagonalizing the energy second-derivatives matrix. To ensure that the transition states were connecting the expected reactants and products, a full optimization of each transition state was done by slightly shifting the geometry of the transition state in either sense following the direction of the transition vector (the eigenvector corresponding to the negative eigenvalue). Diagonalization of the second derivative matrix also provides the vibrational harmonic frequencies used later for the dynamic study. This diagonalization was done both for 1,4-MAT and 1,4-DMAT.

The bulk effect of the solvent was introduced through the isodensity surface-polarized continuum model[23] (IPCM). We used an electronic density of 0.0001 au to define the cavity. The value provided for the dielectric constant was that of 2,2,2-trifluoroethanol (26.5), the most polar solvent used in the experimental study.[24] The IPCM calculations were carried out in both the ground and first triplet electronic states without reoptimization of the geometries.

All the calculations presented here were done with the Gaussian 98 series of programs.[25]

Dynamic Method. Electronic excitation from the ground singlet state (S_0) of 1,4-MAT probably leaves the molecule with some vibrational energy excess above the lowest vibrational level of the first singlet excited state (S_1). After some vibrational relaxation, the molecules populate vibrational states, which make possible the geometries in the region where S_1 and the first triplet electronic state (T_1) potential energy surfaces touch or nearly touch. Then, 1,4-MAT has a nonnegligible probability to jump to an isoenergetic vibrational level of T_1. The lost electronic energy (as T_1 is lower than S_1) is imparted to the nuclei in the form of kinetic energy, in such a way that again an excess of vibrational energy is accumulated. It is not possible to know the energy (E) with which 1,4-MAT will emerge on T_1. However, the hydrogen transfer from ^{3}**K** to ^{3}**E** will occur by quantum-mechanical tunneling only if $E < V^{AG}$, where V^{AG} is the corresponding adiabatic vibrational ground-state energy barrier in the triplet electronic state. As a consequence, we have calculated the rate constants within a range of E values around V^{AG}.

To obtain the microcanonical rate constant including tunneling in the triplet state, we have tried initially to use the following equation due to Miller,[26] which is based on the RRKM theory:[27]

$$k_{QM}(E) = \frac{(m-1)!\prod_{i=1}^{m} h\nu_i}{hE^{m-1}} \sum_{\mathbf{n}} P[E - V^{\ddagger} - \epsilon_n^{vib,\ddagger}] \qquad (1)$$

with

$$\epsilon_{\mathbf{n}}^{vib,\ddagger} = \sum_{i=1}^{m-1} h\nu_i^{\ddagger}\left(n_i + \frac{1}{2}\right) \qquad (2)$$

where m is the number of vibrational degrees of freedom (m = 87 for 1,4-MAT), $\{\nu_i\}$ and $\{\nu_i^{\ddagger}\}$ are respectively the normal-mode frequencies at the reactant molecule and transition state, P is the tunneling probability in the reaction coordinate, $V^{\ddagger}$ is the classical potential energy barrier, and $\mathbf{n} = n_1, n_2, ..., n_{m-1}$ are the vibrational quantum numbers. Indeed, all those magnitudes correspond to the triplet state. Note that

$$V^{AG} = V^{\ddagger} + \sum_{i=1}^{m-1} \frac{1}{2} h\nu_i^{\ddagger} \qquad (3)$$

In the original formulation, the tunneling probability was calculated for a one-dimensional Eckart potential.[28] Instead, we have used here the semiclassical WKB approximation[28] substituting $P[E - V^{\ddagger} - \epsilon_{\mathbf{n}}^{vib,\ddagger}]$ in eq 1 by $P(E,\epsilon_{\mathbf{n}}^{vib,\ddagger})$:

$$P(E,\epsilon_{\mathbf{n}}^{\mathrm{vib},\ddagger}) = \begin{cases} 0 & E < E_0 \\ \dfrac{1}{1+e^{2\theta(E)}} & E_0 < E \le V^{\ddagger} + \epsilon_{\mathbf{n}}^{\mathrm{vib},\ddagger} \\ 1 - P[2(V^{\ddagger} + \epsilon_n^{\mathrm{vib},\ddagger}) - E] & V^{\ddagger} + \epsilon_n^{\mathrm{vib},\ddagger} \le E \le 2(V^{\ddagger} + \epsilon_{\mathbf{n}}^{\mathrm{vib},\ddagger}) - E_0 \\ 1 & 2(V^{\ddagger} + \epsilon_{\mathbf{n}}^{\mathrm{vib},\ddagger}) - E_0, E \end{cases} \quad (4)$$

where E_0 is the energy of the ground vibrational state of 1,4-MAT in the triplet state (the hydrogen transfer is exoergic), and $\theta(E)$ is the classical action integral through the barrier:

$$\theta(E) = \frac{1}{\hbar}\int_{s_1}^{s_2} \sqrt{2[V(s) + \epsilon_{\mathbf{n}}^{\mathrm{vib},\ddagger} - E]}\, \mathrm{d}s \quad (5)$$

where s is the arc length along the reaction path in mass-weighted Cartesian coordinates, s_1 and s_2 are the classical turning points at energy E, and $V(s)$ is the classical potential energy (that is, without the zero-point energy correction) along the reaction path in the triplet state. This reaction path was built up by means of a linear interpolation in mass-weighted Cartesian coordinates linking the transition-state structure with the reactant structure (the **^{3}K** minimum energy structure), and then with the product structure (the **^{3}E** minimum energy structure). Several single-point energy calculations where necessary to obtain an energy profile of $V(s)$ so that, the integral in eq 5 could be calculated numerically through a Simpson method.

In eq 5 we have always used the transition state frequencies $\{\nu_i^{\ddagger}\}$ to evaluate the vibrational energy contribution. Although we realize that vibrational frequencies corresponding to the normal modes, which are orthogonal to the reaction path, depend on s, we assume that in the threshold region where tunneling is important those frequencies are not very different from the ones corresponding to the transition state.

The problem with eq 1 is that it involves summations of all possible vibrational quantum numbers.[29] In the case of sizable molecules such as 1,4-MAT, this implies 86 summations that become computationally unaffordable. Then, we have used the concept of density of states for vibrational modes, $\rho(E_{\mathrm{vib}})$, to substitute the multiple summations in eq 1 by just one summation over E_{vib}, the energy distributed in transition-state vibrational modes. We have employed the classical density of states for the harmonic oscillator to evaluate $\rho(E_{\mathrm{vib}})$. Although this implies the neglect of quantization of the vibrational energy levels, the huge amount of vibrational modes in 1,4-MAT makes this approximation reasonable in practice. So, the microcanonical rate constant including tunneling is finally calculated by

$$k_{\mathrm{QM}}(E) = \frac{(m-1)\prod_{i=1}^{m}\nu_i}{E^{m-1}\prod_{i=1}^{m-1}\nu_i^{\ddagger}} \sum_{E_{\mathrm{vib}}} P(E,E_{\mathrm{vib}})E_{\mathrm{vib}}^{m-2}\Delta E_{\mathrm{vib}} \quad (6)$$

where ΔE_{vib} is the vibrational energy increment and $P(E,E_{\mathrm{vib}})$ is obtained from eqs 4 and 5 by substituting $\epsilon_n^{\mathrm{vib},\ddagger}$ by E_{vib}. Indeed, the lower limit of the summation in eq 6 is the zero-point energy of the transition state (the summation of the second term in eq 3).

For the sake of comparison we have also calculated the classical microcanonical rate constant (that is, without tunneling) k_{clas}. To this aim, in eq 6 we have substituted the tunneling probability given in eq 4 by the classical expression:

$$P(E,E_{\mathrm{vib}}) = \begin{cases} 0 & E < V^{\ddagger} + E_{\mathrm{vib}} \\ 1 & E \ge V^{\ddagger} + E_{\mathrm{vib}} \end{cases} \quad (7)$$

The dynamic calculations were repeated for 1,4-DMAT, whose normal-mode frequencies and tunneling probabilities are different from the ones corresponding to the 1,4-MAT, so causing the KIE.

In this paper we have not taken into account the effect of the rotational degrees of freedom when calculating the rate constant, in such a way that eq 6 corresponds to a total angular momentum null. This should not affect the KIE in a significant way.

Results and Discussion

As in the preceding section, we present first the electronic structure results of *o*-methylanthrone and later on the dynamic results such as the rate constants of 1,4-MAT and 1,4-DMAT and the corresponding kinetic isotope effect.

Electronic Structure Results. Figure 1 depicts the energy profile for the proton-transfer processes. As can be seen, proton transfer should not occur in the ground state because of the large endothermicity of 39.11 kcal/mol and the huge energy barrier of 43.11 kcal/mol for the process. Conversely, on the triplet surface an inversion of relative tautomeric stability is shown, so that now the enol tautomer is more stable than the keto one by 4.36 kcal/mol. This fact makes the proton-transfer reaction in T_1 more likely. Hence, from the triplet-state minimum energy geometry, the energy barrier to overcome is only 7.68 kcal/mol. We have also evaluated the effect of the solvent in the energy profiles using the continuum IPCM method as described in the methodological section. Results of the IPCM calculations are given in Figure 1 inside parentheses. The energies are somewhat different from the isolated (gas phase) ones but no major changes are seen so that the basic picture of the reaction remains unchanged.

A molecular orbital analysis of both minima, **^{3}K** and **^{3}E**, reveals the presence of a crossing of diabatic states along the T_1 proton-transfer process. The lowest energy configurations for **^{3}K** and **^{3}E** minima correspond to n,π^* and π,π^* configurations, respectively. Our results also indicate that this crossing is taking place around the saddle-point region, as a mixture of both n,π^* and π,π^* characters have been found for the electronic configuration at the transition-state structure. Again this picture is not modified when the solvent effect is included. It should be noted that our theoretical results are somewhat different from the predictions made by Garcia-Garibay and co-workers[17] assuming that the keto structure of T_1 corresponds to a mixture of n,π^* and π,π^* excitations, the π,π^* character being the dominant when a more polar solvent was used. Our results indicate that, regardless of the environment, such a mixing only occurs in the transition state region.

Analysis of the geometries of the stationary points corresponding to the proton transfer in both the ground and first triplet electronic states (S_0 and T_1, respectively) reveals the presence of a symmetry molecular plane. Curiously enough, the transferring hydrogen does not belong to the symmetry plane. Conversely, this symmetry plane is not present in the enol form so that the transition state also shows the loss of this plane. Also, it is noteworthy the change in the distance of the C−C bond that involves the methyl group from which the hydrogen transfer takes place, which is followed by a change in the dihedral angle of the methyl hydrogens that gets close to 120°. On the ground state this change in distance goes from 1.51 Å in the keto form, passing the transition-state structure with 1.42 Å, to 1.37 Å in the enol form. But on the triplet state this change in distance is

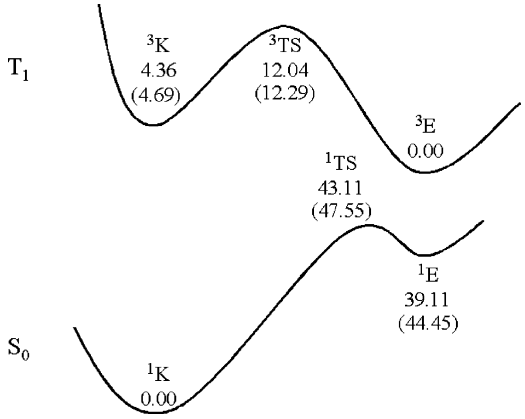

Figure 1. Energy profiles of the proton-transfer reaction coordinate for 1,4-dimethylanthrone in the ground and triplet states. Values in parentheses include the solvent effect.

reduced and goes from 1.51 Å in the keto form to 1.42 Å in the enol form, through a value of 1.49 Å in the transition state. This shortening of the carbon−carbon bond is a direct consequence of the hydrogen transfer. That is, the methyl group becomes a methylene group. This change in distance is less relevant in the triplet-state structures than in the ground-state ones so that this carbon−carbon bond of the enol form in the ground state has a stronger double bond character than in the triplet state. Concomitantly with that fact, the C−O distance of the initial keto structure increases when the oxygen atom receives the proton, the change being again less noticeable in T_1.

Related to the reaction coordinate, which essentially consists of the proton motion, the changes in distance between the carbonylic oxygen and the transferring hydrogen in the ground-state go from 2.47 Å in the keto form through a value of 1.12 Å at the transition-state structure to 0.98 Å in the final enol tautomer. In the triplet state this distance changes from 2.44 Å in the keto form to 1.24 Å in the transition state and, finally, 0.97 Å in the enol tautomer.

It is interesting to note that the initial electronic excitation in 1,4-MAT does not facilitate the proton-transfer reaction. In fact, the n $\rightarrow \pi^*$ excitation withdraws electronic density from the proton-acceptor oxygen atom (where the n orbital is mainly located) so that, tautomerization is disfavored. In fact, the Mulliken population analysis quantifies this change with values of −0.51 and −0.34 au for the proton-acceptor oxygen in S_0 and T_1, respectively. Conversely, the charges on the donor-carbon and transferring hydrogen do not change noticeably upon electronic excitation. The reason the proton transfer is easier in T_1 is the presence of a crossing with the π,π^* state, as this excitation does not affect oxygen but withdraws electronic density from the transferring hydrogen, making it more likely to transfer to the proton-acceptor oxygen atom.

Dynamic Results. We are now ready to analyze the proton-transfer reaction in the lowest triplet state T_1. As this state can only be obtained upon ISC from the singlet excited state initially obtained upon irradiation, a priori it is not possible to know the exact point of the triplet state potential energy surface that will be accessed. Also in this situation of nonequilibrium, temperature cannot be defined so that a calculation of the rate constant can only be done at the microcanonical level. That is, we have to calculate the rate constant at a given energy $k(E)$.

The initial photoexcitation leads the system to the first excited singlet state (S_1). We have calculated the energy corresponding to the vertical excitation from the minimum in the ground state to S_1. This Franck−Condon structure is 14.13 kcal/mol above

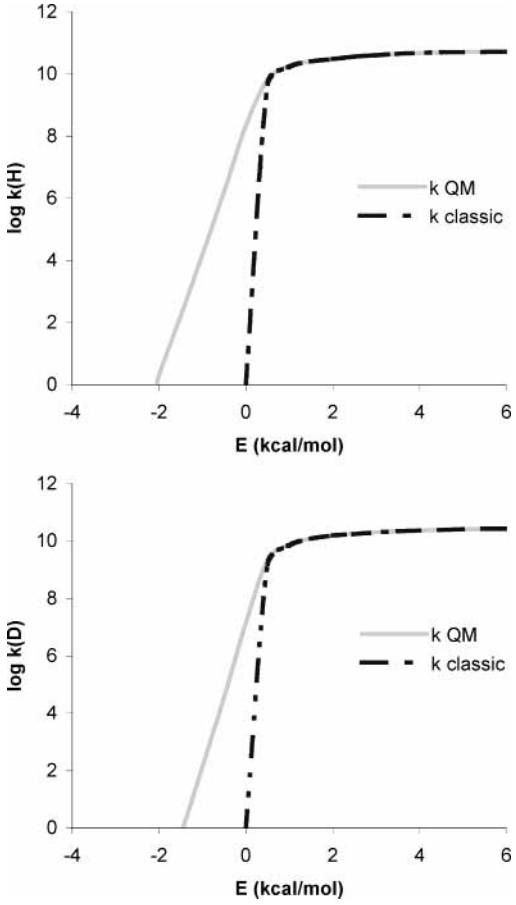

Figure 2. Graphical presentation of the logarithm of microcanonical rate constant (solid) and classical rate constant (dashed) for 1,4-dimethylanthrone (top) and 1,4-dimethylanthrone-d_8 (bottom) as a function of the energy.

the T_1 keto minimum and also well above the energy of the transition state structure for the tautomerization in T_1 (6.45 kcal/mol). So it is quite clear that upon intersystem crossing the structure may still possess enough energy to overcome the transition-state barrier and the excited-state proton transfer will occur. But we should also consider the situation when energy is not enough to overcome the adiabatic barrier and proton transfer takes place through quantum tunneling. To analyze all the possibilities, the classical RRKM theory, adapted to take into account tunneling, has been used as described in the methodological section to evaluate the rate constant at a wide range of available energies.

The obtained rate constants are depicted in Figure 2. Both the perprotio (1,4-MAT, Figure 2, top) and the deuterated (1,4-DMAT, Figure 2, bottom) species are considered as in the experimental data. We have only considered the gas phase energy profile. The energy in the plots is given relative to the transition-state structure for each isotopomer. It includes also the zero point energy so that a positive energy corresponds to an over-the-barrier process, whereas at negative energies the only operative mechanism for the reaction is through quantum tunneling. This explains the main difference between classic and quantum RRKM results shown in Figure 2 as the former suddenly fall to zero at negative energies whereas the quantum rates show a more progressive decay, tunneling becoming less probable as the energy goes further below the threshold. As the energy goes above the adiabatic barrier, both curves quickly merge so that tunneling is not playing any role when the energy is just one kcal/mol above the barrier. Of course this result

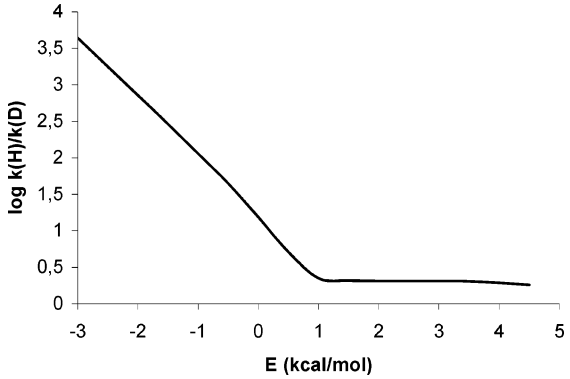

Figure 3. Kinetic isotope effect (KIE) in logarithmic scale as a function of the energy.

appears, in part, as a result of the statistical nature of the RRKM theory that does not take into acccount the actual mechanism of energy transfer between the different degrees of freedom. A more elaborated treatment taking in consideration the dynamics of the energy transfer between the different degrees of freedom would probably show that tunneling is still noticeable at energies slightly above the adiabatic barrier.

It is also to be noted that tunneling is not important when the energy is more than 0.5 kcal/mol below the transition state. This means that the only relevant zone of the reaction path is reduced to the neighbouring of the transition state. Therefore the use of transition-state frequencies as constant values does not imply significant errors.

A simple visual comparison between the 1,4-MAT and 1,4-DMAT rate constants depicted in Figure 2 reveals a clear difference between both isotopomers: the rate constant for the deuterated species decreases more rapidly at negative energies. To obtain a more clear comparison, it is necessary to evaluate the kinetic isotope effect (KIE) by dividing the values of the two rate constants at any given energy. The obtained results are depicted in Figure 3. We have only considered the quantum rate constants as these are the values actually predicted by our calculations. The decrease of tunneling of the deuterated species was, of course, to be expected given the higher mass of the transferring atom. When tunneling is not important, at positive energies, the KIE remains almost invariant taking a limit value of around 2. This value comes from the modification of the normal vibrational modes upon isotopic substitution. At negative energies the KIE rapidly increases so that at 2 kcal/mol below the barrier the KIE is already higher than 10^3.

From the obtained rate constants and the resulting KIEs, it is now possible to compare with the previous experimental data of Garcia-Garibay and co-workers.[17] One of the most striking results was the huge KIE predicted for the reaction of 10^3 or higher. This value is obtained from estimated rate constants k_H and k_D of 10^7 and 10^3 s^{-1}, respectively. Analysis of the results depicted in Figures 2 and 3 reveals that a rate constant of 10^7 s^{-1} for 1,4-MAT is obtained at energies slightly below the adiabatic barrier (around -0.5 kcal/mol). At these energies, the rate for the deuterated species is approximately 10^5 so that the KIE is around 10^2. Of course, given the approximations of our calculations, an exact match between our results and the experimental ones is not expected but the comparison clearly points to the proton-transfer reaction taking place, as expected, through tunneling. However, our results also indicate that the system energy is not far away from the classical energy threshold. At lower energies the KIE would rapidly increase (note the use of a logarithmic scale for the KIE in Figure 3) but the rate constants would become too low to be experimentally measured. On the other hand, at higher available energies, as the adiabatic energy barrier is surpassed, the isotope effect rapidly reaches the limit value given by the frequency changes upon isotopic substitution (in this case around 2.0 as commented above).

Once proton transfer in T_1 is over, another intersystem crossing has to take place to decay to the ground state singlet enol structure. Once on the ground state, the enol structure will easily revert to keto tautomer by a back proton transfer because of the quite low barrier ($\leq$4 kcal/mol) and high exothermicity of the process.

Conclusions

Electronic calculations on the tautomerization of 1,4-dimethylanthrone (1,4-MAT) and its isotopomer 1,4-dimethylanthrone-d_8 (1,4-DMAT) for both the singlet ground state (S_0) and the first triplet state (T_1) reveal that tautomerization is very unlikely in S_0 but energetically favored in T_1 where a barrier of only 7.68 kcal/mol has to be surpassed from the minimum energy structure. In any case, T_1 can only be accessed from S_0 after photoexcitation to a higher singlet excited state (probably S_1) followed by vibrational relaxation and intersystem crossing with T_1. A calculation of the energy of the first singlet excited state at the geometry of the minimum in S_0 (Franck−Condon transition) puts the molecule 6.45 kcal/mol above the transition state structure for the tautomerization in T_1. As it is not possible to know the exact point (below that energy) where the singlet−triplet crossing takes place, purely electronic calculations cannot tell us whether the reaction in T_1 will be possible as an over-the-barrier process or it will take place through quantum tunneling.

A dynamic calculation of the microcanonical rate constant, using a modified RRKM formalism that takes into account the tunneling of the transferring hydrogen, has revealed that the rate constant rapidly decreases as energy goes below the barrier. However, the experimental proposed values of the rate constants for 1,4-MAT and 1,4-DMAT and the predicted large kinetic isotope effect of 10^3 for this reaction can only be explained if the proton transfer takes place through tunneling at an energy only slightly below the adiabatic barrier. Then our dynamic calculations provide an explanation to the lack of phosphorence emission experimentally observed for 1,4-MAT and the large kinetic isotope effect measured for the deuterated 1,4-DMAT.

Acknowledgment. We are grateful for financial support from the Spanish "Ministerio de Ciencia y Tecnología" and the "Fondo Europeo de Desarrollo Regional" through project No. BQU2002-00301, and the use of the computational facilities of the CESCA.

References and Notes

(1) Michl, J.; Bonačić-Koutecký, V. *Electronic Aspects of Organic Photochemistry*; John Wiley and Sons: New York, 1990.

(2) Turro, N. J. *Modern Molecular Photochemistry*; Benjamin Cummings Publishing Co.: Menlo Park, CA, 1978.

(3) Porter, G.; Tchir, M. F. *J. Chem. Soc., Chem. Commun.* **1970**, 1372−1373.

(4) Haag, R.; Wirz, J.; Wagner, P. J. *Helv. Chim. Acta* **1977**, *60*, 2595−2607.

(5) Das, P. K.; Encinas, M. V.; Small, R. D., Jr.; Scaiano, J. C. *J. Am. Chem. Soc.* **1979**, *101*, 6965−6970.

(6) Scaiano, J. C. *Chem. Phys. Lett.* **1980**, *73*, 319−322.

(7) Ito, Y.; Inada, N.; Matsuura, T. *J. Chem. Soc., Perkin Trans. 2* **1983**, 1857−1861.

(8) Nakayama, T.; Hamanoute, K.; Hidaka, T.; Okamoto, M.; Terenashi, H. *J. Photochem.* **1984**, *24*, 71−78.

(9) Findlay, D. M.; Tchir, M. F. *J. Chem. Soc., Faraday Trans. 1* **1976**, *72*, 1096−1100.

(10) Kumar, C. V.; Chattopadhyay, S. K.; Das, P. K. *J. Am. Chem. Soc.* **1983**, *105*, 5143−5144.

(11) Redmond, R. W.; Scaiano, J. C. *J. Phys. Chem.* **1989**, *93*, 5347−5349.

(12) Akiyama, K.; Ikegami, Y.; Tero-Kubota, S. *J. Am. Chem. Soc.* **1987**, *109*, 2538−2539.

(13) Garcia-Garibay, M. A.; Gamarnik, A.; Pang, L.; Jenks, W. S. *J. Am. Chem. Soc.* **1994**, *116*, 12095−12096.

(14) Garcia-Garibay, M. A.; Gamarnik, A.; Bise, R.; Pang, L.; Jenks, W. S. *J. Am. Chem. Soc.* **1995**, *117*, 10264−10275.

(15) Johnson, B. A.; Gamarnik, A.; Garcia-Garibay, M. A. *J. Phys. Chem.* **1996**, *100*, 4697−4700.

(16) Garcia-Garibay, M. A.; Jenks, W. S.; Pang, L. *J. Photochem. Photobiol. A* **1996**, *96*, 51−55.

(17) Gamarnik, A.; Johnson, B. A.; Garcia-Garibay, M. A. *J. Phys. Chem. A* **1998**, *102*, 5491−5498.

(18) Francl, M. M.; Pietro, W. J.; Hehre, W. J.; Binkley, J. S.; Gordon, M. S.; DeFrees, D. J.; Pople, J. A. *J. Chem. Phys.* **1982**, *77*, 3654.

(19) (a) Lee, C.; Yang, W.; Parr, R. G. *Phys. Rev. B* **1988**, *37*, 785. (b) Becke, A. D. *J. Chem. Phys.* **1993**, *98*, 5648.

(20) Casida, M. E.; Jamorski, C.; Casida, K. C.; Salahub, D. R. *J. Chem. Phys.* **1998**, *108*, 4439.

(21) Stratmann, R. E.; Scuseria, G. E.; Frisch, M. J. *J. Chem. Phys.* **1998**, *37*, 785.

(22) Peng, C.; Ayala, P. Y.; Schlegel, H. B.; Frisch, M. J. *J. Comput. Chem.* **1996**, *17*, 49.

(23) Foresman, J. B.; Keith, T. A.; Wiberg, K. B.; Snoonian, J.; Frisch, M. J. *J. Phys. Chem.* **1996**, *100*, 16098.

(24) Weast, R. C., Ed.; *Handbook of Chemistry and Physics*; The Chemical Rubber Co.: Cleveland, OH, 1970.

(25) Frisch, M. J.; Trucks, G. W.; Schlegel, H. B.; Scuseria, G. E.; Robb, M. A.; Cheeseman, J. R.; Strain, M. C.; Burant, J. C.; Stratmann, R. E.; Dapprich, S.; Kudin, K. N.; Millam, J. M.; Daniels, A. D.; Petersson, G. A.; Montgomery, J. A.; Zakrzewski, V. G.; Raghavachari, K.; Ayala, P. Y.; Cui, Q.; Morokuma, K.; Foresman, J. B.; Cioslowski, J.; Ortiz, J. V.; Barone, V.; Stefanov, B. B.; Liu, G.; Liashenko, A.; Piskorz, P.; Chen, W.; Wong, M. W.; Andres, J. L.; Replogle, E. S.; Gomperts, R.; Martin, R. L.; Fox, D. J.; Keith, T.; Al-Laham, M. A.; Nanayakkara, A.; Challacombe, M.; Peng, C. Y.; Stewart, J. P.; Gonzalez, C.; Head-Gordon, M.; Gill, P. M. W.; Johnson, B. G.; Pople, J. A. *Gaussian98*; Gaussian Inc.: Pittsburgh, PA, 1998.

(26) Miller, W. H. *J. Am. Chem. Soc.* **1979**, *101*, 6810−6814.

(27) Steinfeld, J. I.; Francisco, J. S.; Hase, W. L. *Chemical Kinetics and Dynamics*; Prentice Hall: Englewood Cliffs, NJ, 1989.

(28) Bell, R. P. *The Tunnel Effect in Chemistry*; Chapman and Hall: New York, 1980.

(29) Zhang, S.; Truong, T. N. *J. Phys. Chem. A* **2001**, *105*, 2427−2434.